Fall 2011

Processing and mechanical characterization of polyurea aerogels

Jared M. Loebs

Department:

PROCESSING AND MECHANICAL CHARACTERIZATION OF POLYUREA AEROGELS

by

JARED MICHAEL LOEBS

A THESIS

Presented to the Faculty of the Graduate School of the

MISSOURI UNIVERSITY OF SCIENCE AND TECHNOLOGY

In partial Fulfillment of the Requirements for the Degree

MASTER OF SCIENCE IN MECHANICAL ENGINEERING

2011

Approved by

Lokeswarappa Dharani
Nicholas Leventis
Jeffery Thomas

ABSTRACT

The use of aerogels historically has been limited to extreme cases largely in part to the nature of their mechanical properties. Until recently many aerogels produced have been brittle and weak, though looking at their specific strength would suggest otherwise. This thesis outlines the processing and major mechanical properties of a relatively new type of aerogel, polyurea aerogel, that shows promise in a variety of fields including structures.

Processing polyurea aerogel begins with a liquid solution that solidifies to form a solid gel filled with liquid that is later removed by supercritical drying. Once dry, polyurea aerogels are difficult to form by standard methods such as machining without damaging the surface of the material. Because of this, methods of mold-making have been investigated to form the gel into an appropriate size and shape before the solid structure forms. It has been found that polypropylene plastic can resist the chemicals used during the manufacturing process while still being inexpensive and easy to work with.

Testing has been conducted in tension, compression, bending, shear, and toughness for densities of polyurea aerogels ranging from 0.12 g/cm^3 to 0.31 g/cm^3. In most cases the strength is found to be similar to other building materials of the same density, such as balsa wood, except in the axial compression direction. After undergoing strain hardening up to approximately 40-50%, polyurea aerogel strength increases exponentially and a specific failure point is difficult to determine.

ACKNOWLEDGMENTS

I would like to express my deepest gratitude to the people that made this project possible. First and foremost I acknowledge my advisors, Drs. Lokeswarappa Dharani and Nicholas Leventis, their guidance and insight have kept this project alive and on track. Dr. Jeffery Thomas has been kind and helpful in every meeting we've had, providing not only a lab and support to test the mechanical properties found in this paper but also knowledge and wisdom he has gathered from his experiences testing similar properties of many different materials. Ph.D candidates Chakkaravarthy Chidambareswarapattar and Dhairyashil Mohite have provided a knowledge of chemistry far beyond what my mind is capable of understanding and have both been the greatest of help in the Leventis Lab keeping a watchful eye on this fish out of water (or rather, mechanical engineer in a chemistry lab). Fellow student of Mechanical Engineering, Zachery Larimore, was kind enough to pass down his knowledge of manufacturing and working with polyurea and other aerogels which saved me a semester's worth of trial and error, and I owe him much.

The Army Research Office has funded this research. Without their support this research would not have been possible.

Finally, my family and friends, especially Ashley Baechle and Tyler Fears, have supported me throughout my six years in Rolla and motivated me to continue pressing on.

TABLE OF CONTENTS

LIST OF ILLUSTRATIONS

LIST OF TABLES

1. INTRODUCTION

1.1. GENERAL

An aerogel is a solid material characterized by its low density and high porosity and surface area.[1,2] Although the term “aerogel” conjures thoughts of modern high performance materials, the truth is that they were first created in the late 1920's or early 1930's (the exact date is open to debate) by Kistler.[3] He wanted to show that the continuous solid structure found in a wet gel could be kept if the liquid in the wet gel was removed. Initial attempts to create aerogels involved allowing the solvent to evaporate; however, this led to structural failure in the material due to surface tension between the evaporating liquid trying to escape and the original structure. It became apparent that a method of manufacture was necessary in which the liquid solvent was removed all at once. In Kistler's own words,

> Obviously, if one wishes to produce an aerogel, he must replace the liquid with air by some means in which the surface of the liquid is never permitted to recede within the gel. If a liquid is held under pressure always greater than the vapor pressure, and the temperature is raised, it will be transformed at the critical temperature into a gas without two phases having been present at any time." [3]

This process, known as supercritical drying, was first attempted using water as a solvent while trying to create silica aerogels.[4] It was found that the supercritical water dissolved the silica thus destroying the structure. The process was then modified by replacing the water with alcohol through a series of solvent exchanges. The fix worked, and the first aerogels were born.

Aerogels created from silica exhibited very low thermal, electric, and acoustic conductivity.[5,6,7] One major drawback of these aerogels was their poor mechanical properties including strength and toughness.[8,9] Because they were so brittle their use was limited to applications such as in nuclear reactors or Cerenkov reactors and spacecraft insulation.[6,5] This problem was remedied by coating the microstructure with a conformal polymer layer, resulting in a slight (~3x) increase in density, increased flexibility, over 100x increase in strength, making it feasible to use aerogels in structural applications.[5,10,11] In a similar vein, aerogels have been created with a microstrucure consisting entirely of polymer, such as polyurea, which is the main topic of this paper.

The aerogels discussed in this text were created by the reaction of the triisocyanate Desmodur N3300a and water, catalyzed with triethylamine in a solution of acetone. Since aerogels created in this fashion consist of polyurea, they are referred to as polyurea aerogels, hereafter shortened to PUA. Three examples of PUA have been used in each of the tests described. Though chemically identical, the three examples have been created with varying density. The three densities investigated represent the upper end of densities that can be easily produced. The three densities studied are 0.12 g/cm^3, 0.17 g/cm^3, and 0.31 g/cm^3.

1.2. RESEARCH OBJECTIVE

This project represents the first stage in developing an understanding of the physical properties of PUA. With the data collected in this study it has become possible to propose PUA for use in engineered structures requiring a known amount of mechanical strength and stiffness.

2. FABRICATION METHODS

2.1. GENERAL

Fabrication of samples started with the knowledge that PUA is derived from the mixing of chemical precursors in a solvent. After reacting a wet gel is formed, or an solid porous structure filled with a liquid (as opposed to the desired fill of gas). Finally, the wet gel is put through a process called supercritical drying. In this process the liquid solvent is replaced with liquid carbon dioxide, which is then converted into a supercritical fluid and flashed off into gas.

Completed PUA samples are somewhat difficult to work with.[12] Observations show that the material is more likely to deform or tear when machined or cut with all but the sharpest tools. Because of this, it was decided to manufacture the required specimen shapes early on in the processing phase. A variety of molds were produced and tested in which the liquid PUA was poured into, thus allowing the wet gel to take the desired shape. Considerations had to be made due to the nature of some of the chemicals in use, namely acetone, and how they would react to different mold materials.

2.2. SILICONE MOLDS

The first material used for the manufacture of molds was silicone. It was hoped that a mold made from the flexible silicone would provide an ideal solution to removing the still relatively fragile PUA wet gels with minimal effort and user interaction. Like many epoxy resins, the silicone used for these molds was created by mixing a two part solution of viscous silicone with a hardening catalyst (AeroMarine Silicone RTV

Rubber). Because this material started as a flowing liquid it was necessary to create a mold to pour the solution into. Wax blocks were chosen due to their low cost, ease of machining, and availability. Figure 2.1 shows two examples of machined wax blocks that were used in the process. Notice that the left and lower right machined cavities have been filled with the silicone solution. Figure 2.2 shows the cured silicone molds just after they have been released from the wax blocks.

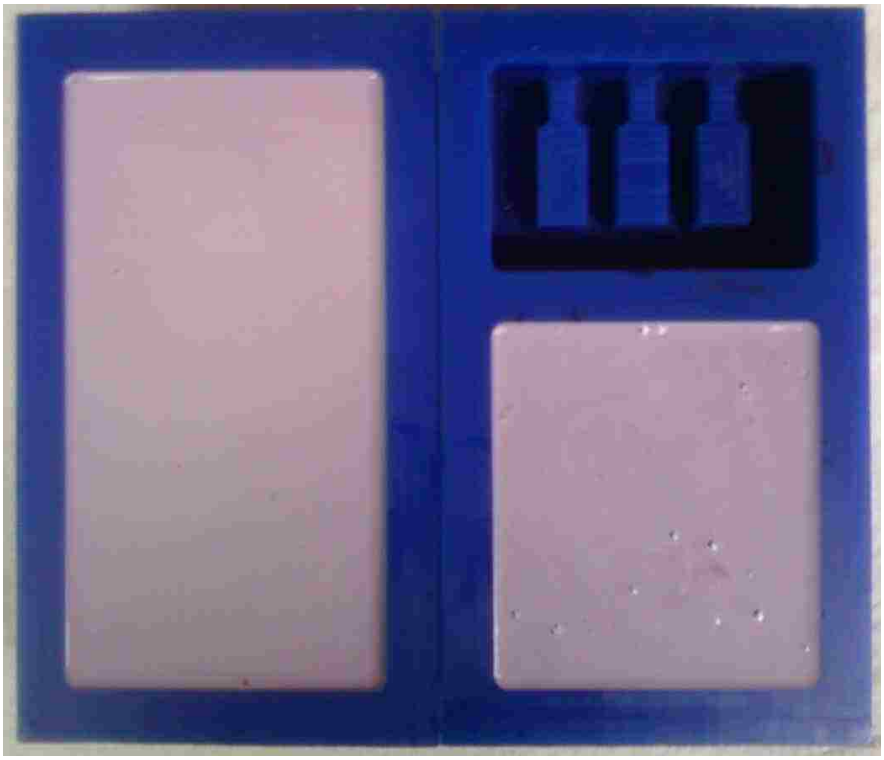

Figure 2.1. Wax Blocks Used as Molds for Pourable Silicone Solution. Wax blocks have been machined to create cavities in the shape of the desired molds. These cavities are then filled with a liquid silicone solution and left to cure overnight.

Figure 2.2. Silicone Molds After Release from Wax Blocks. After being left to cure overnight the (now solid) silicone is removed from the wax blocks. The cured silicone is solid but flexible, allowing easy removal of delicate PUA samples.

Notice from Figure 2.2 that the silicone molds have two open faces; one small opening at the top and the large open face closest to the camera. To complete the mold it was necessary to attach a polypropylene plate to the large open face, thus making a structure that has only one small opening at one end through which the liquid PUA solution could be poured. The finished molds can be seen in Figure 2.3.

Figure 2.3. Finished Silicone Molds. To complete the molds a sheet of polypropylene plastic is fixed to the open face of the silicone molds with rubber bands. This method allowed quick and easy access to samples after they had formed wet gels.

During initial trials it seemed that the PUA wet gels were drying out; that is, the acetone solvent was escaping the molds as vapor leaving the delicate wet gels exposed to air which led to varying degrees of structural collapse. Upon further investigation it was determined that the wet gels were not drying out, but rather acetone was being absorbed into the silicone molds making them swell. This change in size during the gelation of the PUA solution led to problems with the size and quality of the samples produced.

To remedy this problem the silicone molds were pre-soaked in acetone and then returned to their acetone bath after the PUA solution had been poured into them. This setup can be seen in Figure 2.4.

Figure 2.4. Silicone Molds in Acetone Bath. Due to shrinking of the PUA samples within the silicone molds (caused by the absorbtion of acetone from the samples into the silicone) the entire assembly was soaked in acetone prior to and during gelation of PUA.

This setup yielded wet gels that were the correct size and shape but yellow in color (as opposed to the clean white color normally achieved). It was hypothesized that material from the rubber bands holding the polypropylene plate onto the silicone molds was being dissolved in the acetone and flowing into the PUA solution before gelation had occurred. It was found that the rubber bands, which were yellow in color, quickly degraded through washing and drying cycles in acetone. This method of constructing PUA samples was abandoned shortly after the creation of discolored samples for fear that the properties of the finished PUA would be compromised. It was decided to design new molds, this time entirely from polypropylene.

2.3. POLYPROPYLENE MOLDS

Switching mold materials from silicone to polypropylene meant that a new design was necessary that would easily allow the wet gels to be removed from their molds without damage. A mold using a series of plates was imagined in which outer "face" plates, similar to the one used on the silicone mold, would surround one or more plates with cut-outs that incorporated both the filling neck and desired cavity shape. A large 0.25 inch thick sheet of polypropylene was obtained and the University waterjet facility was contacted to make the desired cutouts. Figures 2.5 and 2.6 show the University waterjet and the polypropylene sheet shortly after being cut, respectively.

Figure 2.5. Missouri University of Science and Technology Waterjet. High pressure water is fed through a computer controlled nozzle to machine parts a variety of materials including metal, wood, plastic, and stone.

Figure 2.6. Freshly Cut Polypropylene Sheet. A computer controlled routine was created to cut the required mold-making parts from polypropylene plastic. These parts will be stacked and bolted together to form the new molds.

The plates cut from polypropylene were stacked together in layers and held together by a series of bolts placed around the perimeter of the mold. Slight differences in clamping pressure was observed between the bolts due to the ductility of the polypropylene sheets. This initially caused a small amount of leaking, which was alleviated through the use of washers and a think layer of silicone grease applied between the sheets. An assembled mold can be seen in Figure 2.7.

Figure 2.7. Assembled Polypropylene Mold. Polypropylene sheets have been stacked and bolted together. Openings are left at the top through which solution is poured. Here the outline of the mold cavity is partially visible, revealing the dogbone shape used for tensile testing.

The new molds constructed of polypropylene have been found to easily produce quality PUA samples and were used to construct all samples used for testing.

2.4. SAMPLE PREPARATION

After the wet gels are removed from the molds, they are placed in a supercritical dryer, which through a cycle of washes replaces the acetone in the wet gels with carbon dioxide. Once saturated, the pressurized dryer is heated until the liquid carbon dioxide was converted to a supercritical fluid, that in turn was gradually vented off slowly.

Once successfully dried, PUA samples need very minimal preparation before mechanical testing. In most cases, small outcrops of material are left where the filling neck is located on the mold. These bits of material are easily removed on a belt sander. The samples are then checked for blemishes or visible imperfections (if any were found the sample was disposed of), labeled, measured, and weighed. The recipes used to create the samples have been included in Table 2.1.

Table 2.1. Polyurea Aerogel Recipes

PUA Recipe	N3300A (g)	Acetone (mL)	Water (mL)	Triethylamine (mL)	Linear Shrinkage (%)	Measured Density (g/cm^3)
11g	11	94	1.77	0.38	1.8	0.12
16.5g	16.5	94	1.77	0.38	2.4	0.17
33g	33	94	0.88	0.19	5.2	0.31

It should be noted that the amount of triethylamine added to the mixture has a direct impact on the time it takes the solution to form a solid gel. For both, 0.12 and 0.17 g/cm^3 samples, 0.38 mL of triethylamine was added to achieve a gel time of approximately one hour. 33g recipes created using the same amount of triethylamine had a high probability of forming voids and defects within the samples. In an effort to fix this problem the gel time was increased to approximately four hours by halving the amount of triethylamine and water added. This change in formulation also reduced the amount of shrinkage in the samples to a level similar to that of the other two densities.

2.5. PHYSICAL STRUCTURE OF POLYUREA AEROGEL

The physical microstructure of the three densities being studied are each unique and play a critical role in the strength and stiffness characteristics. Figures 2.8, 2.9, and 2.10 show scanning electron microscope images of all three densities at magnification levels of 300k, 200k, and 100k, respectively.

It can be seen from the SEM images that the 0.12 g/cm^3 PUA forms a network of fibers with large amounts of open space between the fibers. Increasing the density to 0.17 g/cm^3 shows that the structure still consists of areas of open space, though the fibers that were apparent in the lower density have begun to form small particulates along their length. Finally, in the highest density it is apparent that the fibrous structure found in the lower densities has been replaced by particles, and the space between particles is much smaller.

It will be shown later in this thesis that for a given increase in density, the increase in strength and stiffness (especially in shear and compression) is not linear but exponential. This may be attributed to the decrease in open space between particles, leaving less room for the structure to move from its original location.

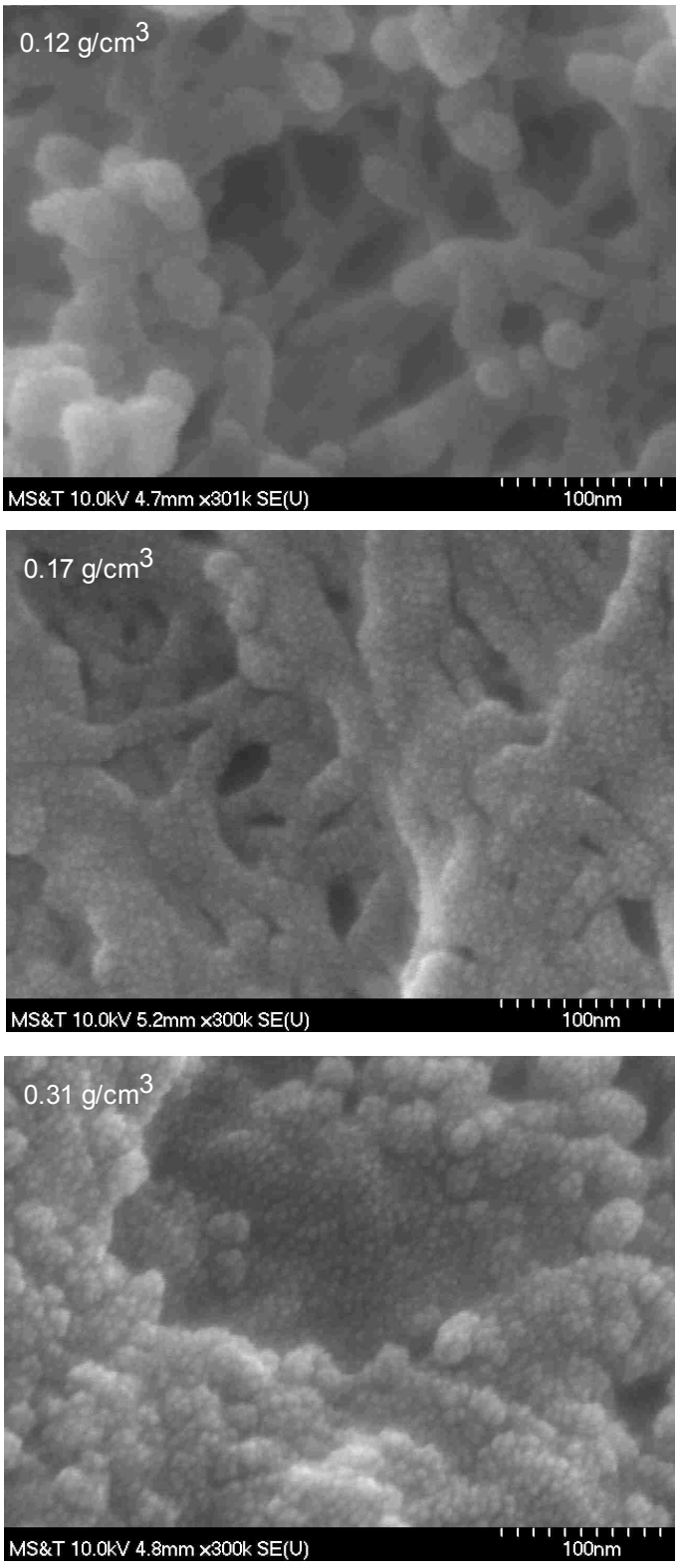

Figure 2.8. SEM Image, 300k x Zoom. Scanning electron microscope pictures have been taken of PUA at a zoom level of 300k times. The top photo shows the microstrucure of 0.12 g/cm^3 PUA, the middle 0.17 g/cm^3, and 0.31 g/cm^3 is on the bottom.

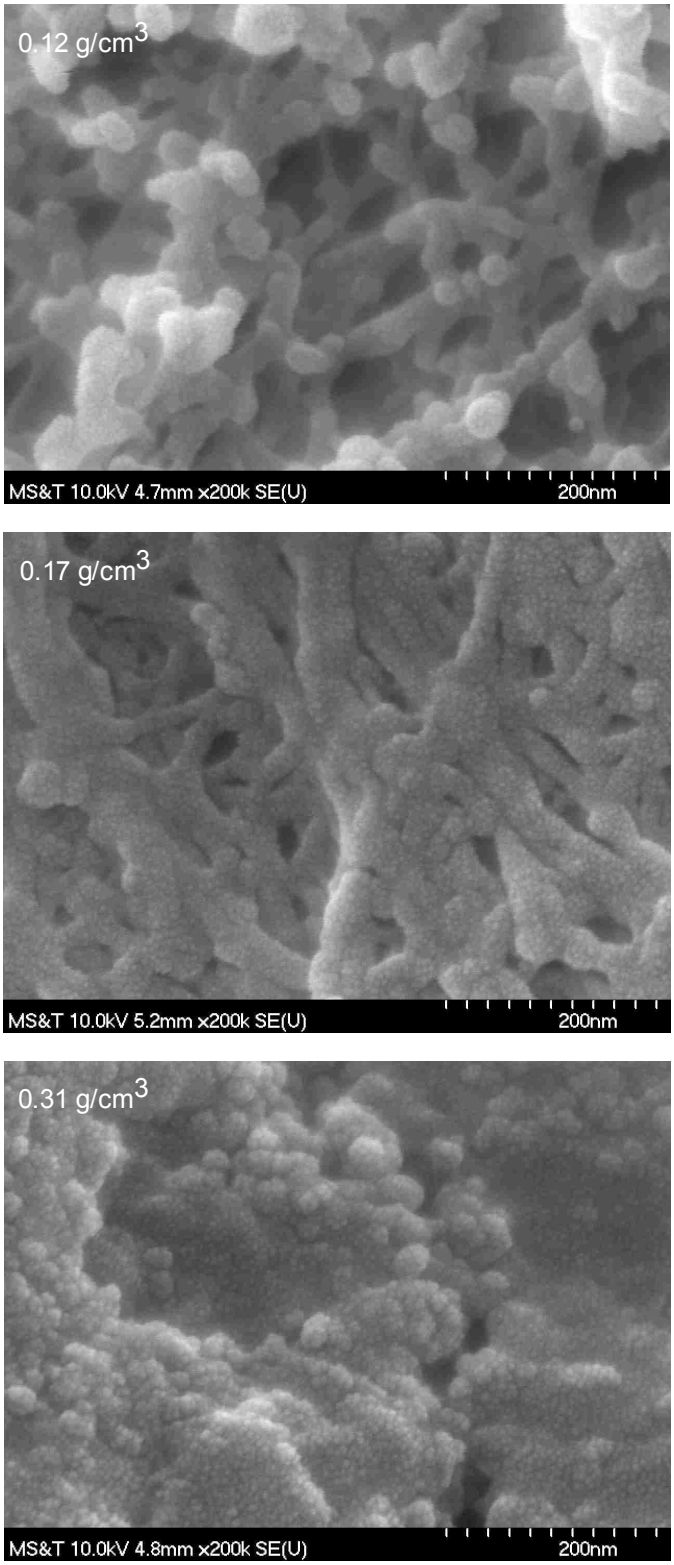

Figure 2.9. SEM Image, 200k x Zoom. Scanning electron microscope pictures have been taken of PUA at a zoom level of 200k times. The top photo shows the microstrucure of 0.12 g/cm^3 PUA, the middle 0.17 g/cm^3, and 0.31 g/cm^3 is on the bottom.

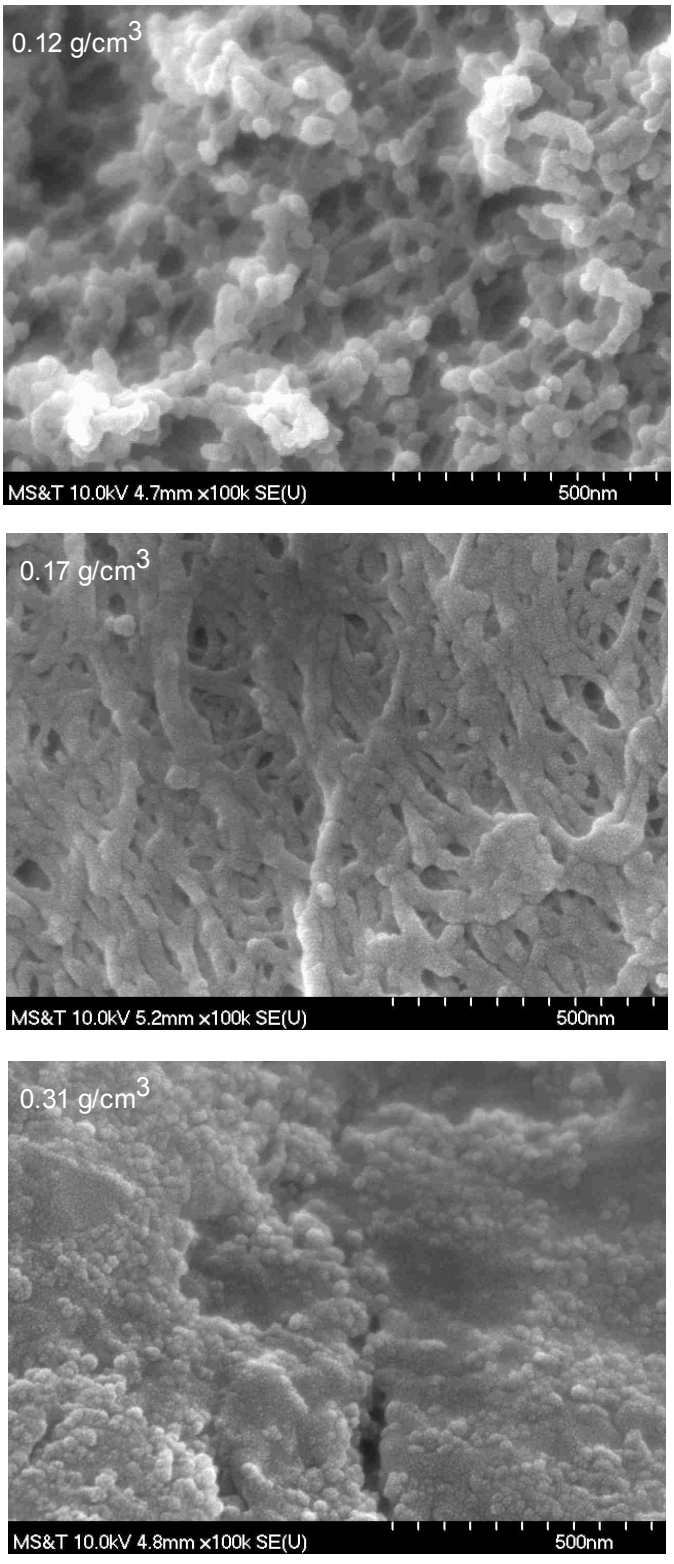

Figure 2.10. SEM Image, 100k x Zoom. Scanning electron microscope pictures have been taken of PUA at a zoom level of 100k times. The top photo shows the microstrucure 0.12 g/cm^3 PUA, the middle 0.17 g/cm^3, and 0.31 g/cm^3 is on the bottom.

3. TESTING

Testing proceeded with the knowledge that mechanical strength needed to be quantified in the tensile, compressive, and shear directions. Determination of the strength in tension and compression was fairly straightforward. Tensile properties were easily determined by pulling a sample apart. Compressive properties were found by compressing a sample. Properties in shear, however, proved more difficult to determine.

Three point bend tests are common and samples are subjected to combined tensile, compressive, and shear forces, though extracting data for properties in any of these directions is difficult due to the ductility and bi-modular characteristics exhibited by PUA. Because of this, a new test was created to put a specimen in pure shear.

With properties in the three main direction known a Charpy impact test was added in an effort to measure the toughness, or the ability to resist a fracture from propagating, of PUA.

3.1. TENSION

ASTM D638 outlines the methods and procedures standardized for testing plastic specimens in tension and has been chosen as a guideline obtaining the tensile properties of PUA. This test specifies the appropriate dimensions of the “dog bone” specimen shape, shown in Figure 3.1. Additionally, five specimens of each density have been tested at a strain rate of two mm/min. All testing has been completed in ambient temperature, pressure, and humidity on an Instron 4469 material testing machine. Figure 3.2 shows a tension dog bone loaded into the machine, ready to test.

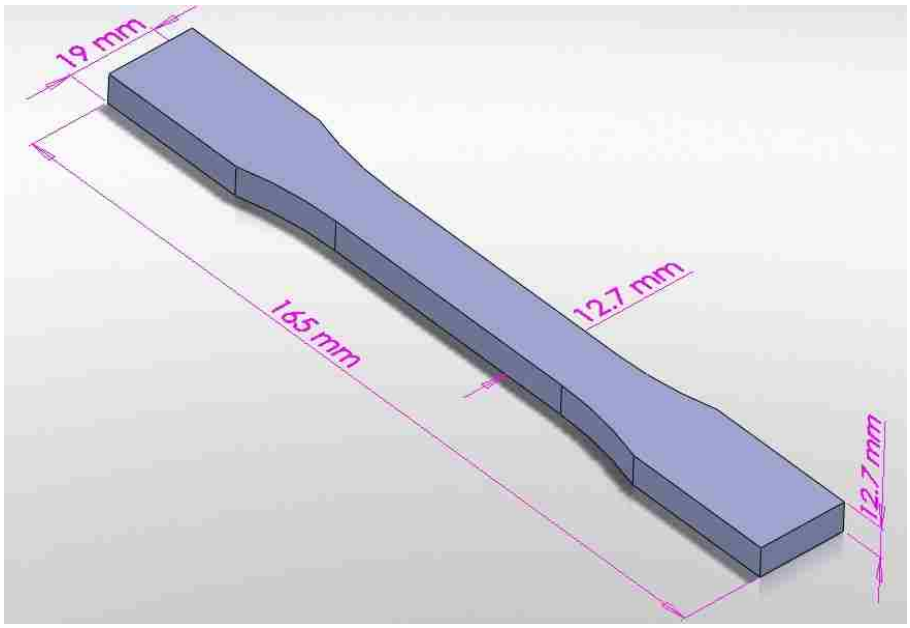

Figure 3.1. Isometric View of Tension Dog Bone. The major dimensions of the dogbone specimen used for tensile testing are shown.

Figure 3.2. Tensile Test Setup. A dogbone specimen is loaded into the Instron material testing machine via two clamps. The lower clamp is stationary and the top clamp is fixed to a load cell mounted on a computer actuated beam. This beam raises and lowers depending on the type of test being conducted.

The results from testing 0.12 g/cm^3, 0.17 g/cm^3, and 0.31 g/cm^3 samples have been analyzed and plotted. Figure 3.3 shows stress-strain curves comparing the three densities of PUA, tested to failure. Figure 3.4 shows stress-strain curves comparing stiffness (low strain, linear elastic region) of the three densities of PUA. Perfectly linear regions of elastic deformation were not present in all tests so stiffness has been calculated using the secant method rather than the more standard 2% yield offset..

It can be seen from the results that as the density increases so does the both the strength and stiffness. This relationship appears to be linear between the two lower densities, meaning that a 50% increase in density results in approximately 50% increase in strength and stiffness, though the relationship becomes exponential when the density is increased to 0.31 g/cm^3. All three densities saw a yield in strength at approximately 3.5% strain, and the 0.12 g/ cm^3 and 0.17 g/ cm^3 densities both failed at around 13%. It should be noted that the 0.31 g/ cm^3 density had an ultimate failure at a much lower strain, approximately 6%. This can most likely be attributed to the differences in microstrucure between the densities (fibrous vs particulate). The results from testing have been tabulated and can be seen in Table 4.1.

Table 4.1. Tensile Testing Results

PUA Density	Young's Modulus (MPa)	Yield Stress (MPa)	Failure Stress (MPa)	Failure Strain (%)
0.12 g/cm^3	24.1 ± 0.5	0.7 ± 0.03	1.1 ± 0.08	12.5 ± 2.3
0.17 g/cm^3	37.2 ± 1.3	1.0 ± 0.2	1.7 ± 0.1	13.5 ± 3.0
0.31 g/cm^3	102 ±7.2	2.93 ± 0.4	3.9 ± 0.2	6.0 ± 0.6

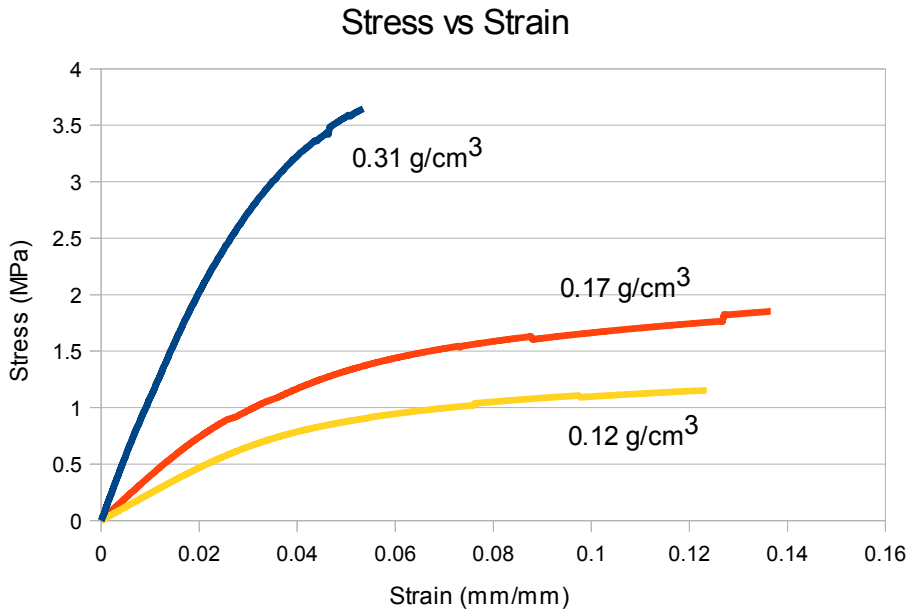

Figure 3.3. Tensile Testing Results. The top (blue) line represents the 0.31 g/cm^3 PUA, the middle (orange) line represents 0.17 g/cm^3, and the bottom (yellow) line represents 0.12 g/cm^3. The strength and stiffness of the 0.31 g/cm^3 PUA is significantly higher than the 0.12 g/cm^3 and 0.17 g/cm^3, though it failed at approximately half of the strain.

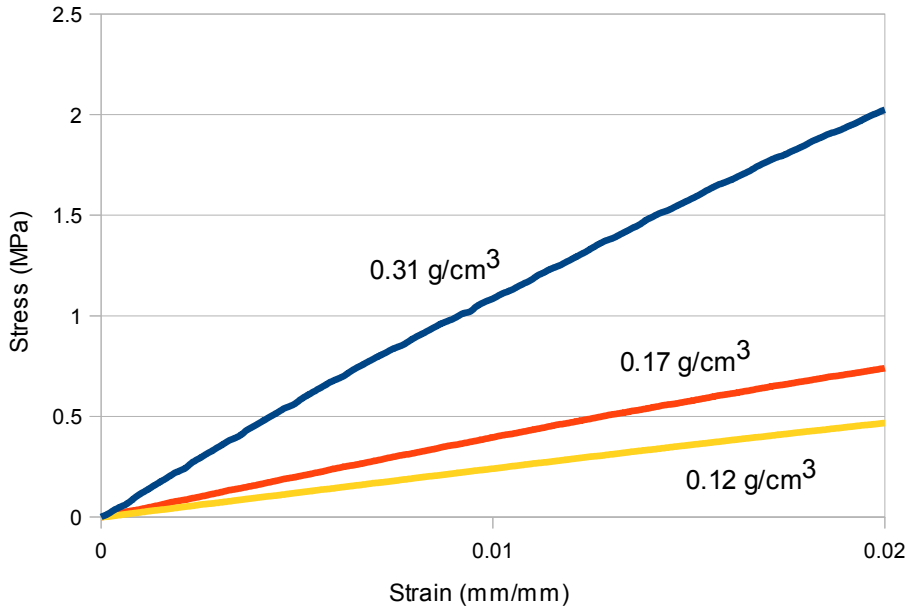

Figure 3.4. Stiffness in Tension Results. The top (blue) line represents 0.31 g/cm^3 PUA, the middle (orange) line 0.17 g/cm^3, and the bottom (yellow) line 0.12 g/cm^3.

3.2. COMPRESSION

ASTM D695 outlines the standardized testing methods for testing rigid plastics in compression and has been used as a guideline for determining the compressive properties of PUA. The rate of testing used is 1.3 mm/min, and is prescribed by the test method. As in the tensile tests, five test specimens have been used to ensure accuracy of the results. The Instron 4469 material testing machine previously shown has been utilized for these tests, which have been conducted at room temperature, pressure, and humidity. The dimensions of the test specimens used for this test are shown in Figure 3.5. Figure 3.6 shows test setup with a sample loaded into the Instron machine.

The results from testing 0.12 g/cm^3, 0.17 g/cm^3, and 0.31 g/cm^3 samples have been plotted and analyzed. Figure 3.7 shows the stress-strain curves for all densities of PUA up to their yield stress, whereas Figure 3.8 focuses on the stiffness. It can be seen that the increase in density affects strength in a similar fashion to what was observed in the tensile testing. Also similar to the tensile testing, all three densities began to yield at approximately 3-4%. What is interesting to note is that none of the densities tested experienced a failure at these strain levels. In search of this failure point the compression tests were continued to higher strain values. Figure 3.9 shows the results for compression testing at these high strain values (50-100%).

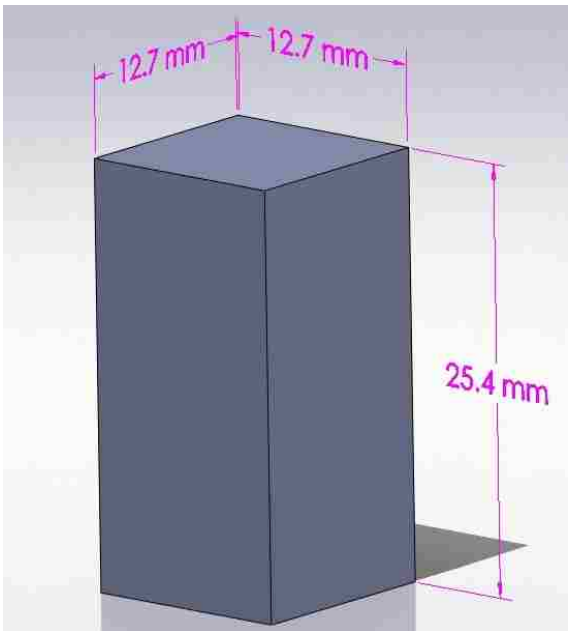

Figure 3.5. Isometric View of Compression Test Sample. The dimensions of the compression test specimen listed in the test method are represented above.

Figure 3.6. Compression Test Setup. The Instron testing machine has been fitted with two plates, one being fixed to a load cell, for the compression tests.

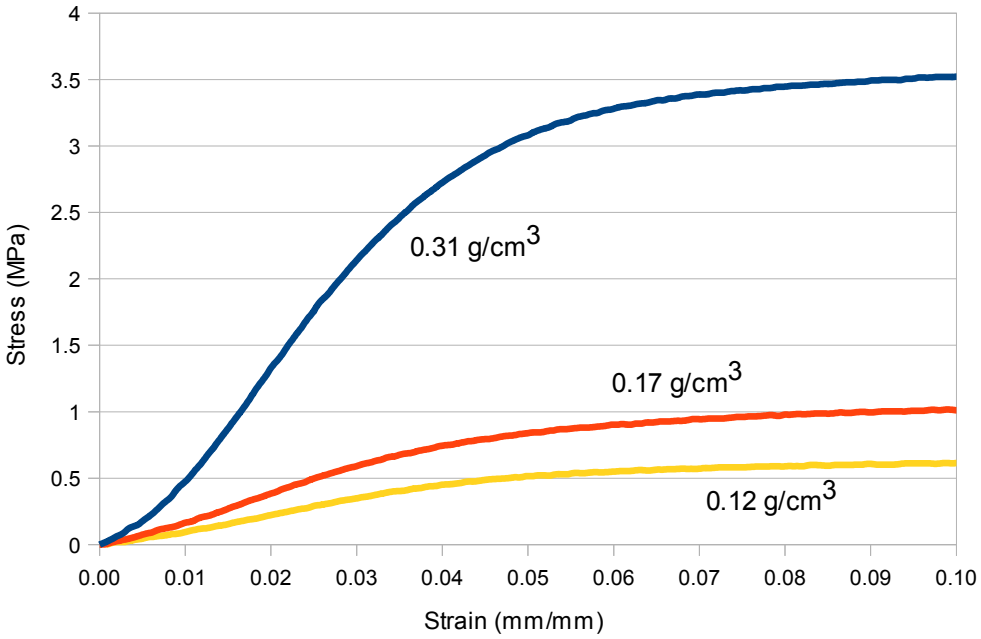

Figure 3.7. Compressive Test Results. The plot above shows the stress-strain curves for PUA. 0.31 g/cm^3 PUA is on top (blue), 0.17 g/cm^3 in the middle (orange), and 0.12 g/cm^3 on the bottom (yellow). Yielding for all densities occurred at approximately 3-4% strain, after which the stress values plateaued.

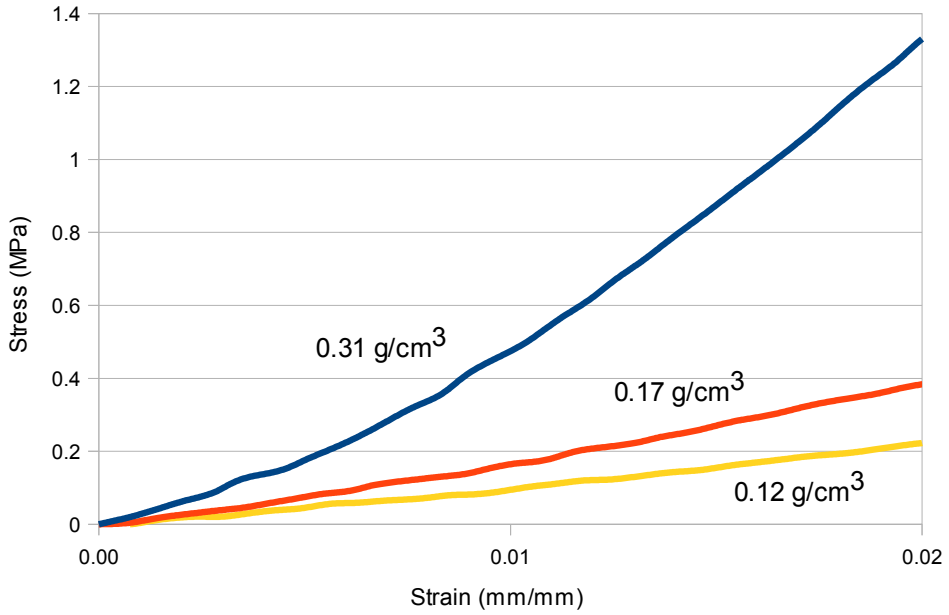

Figure 3.8. Stiffness in Compression Results. 0.31 g/cm^3 results are on top (blue), 0.17 g/cm^3 in the middle (orange), and 0.12 g/cm^3 on bottom (yellow). It can be seen that the increase in density has a very large (positive) effect on material stiffness.

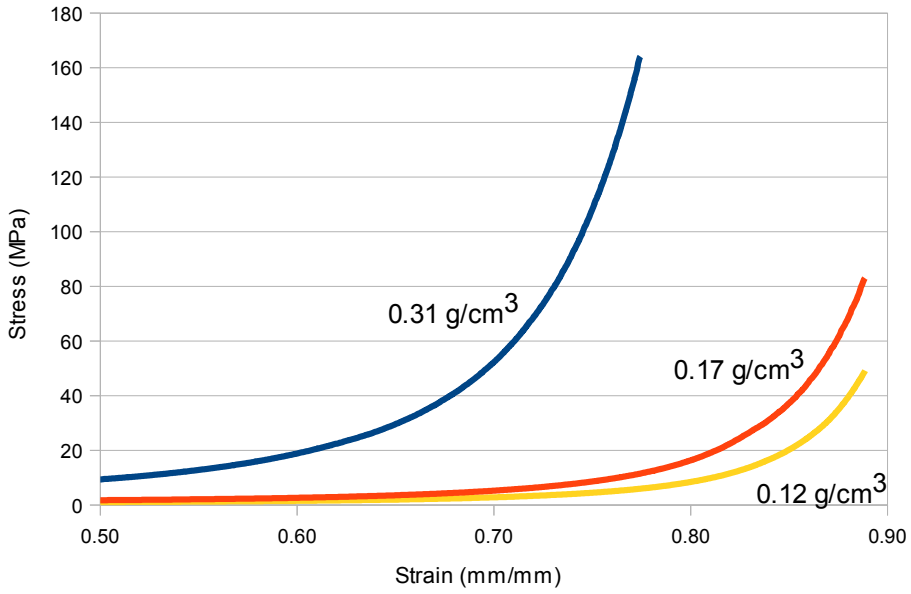

Figure 3.9. High Strain Compression Test Results. Top line (blue) is 0.17 g/cm^3, middle (orange) is 0.17 g/cm^3, and bottom (yellow) is 0.12 g/cm^3. Both lower densities began to increase in strength at approximately the same strain, while the 0.31 g/cm^3 increased significantly earlier.

Even at these increased strain values a failure was difficult to identify. It can be seen from the plots that after reaching a yield point the stress within the PUA samples leveled out until strain values of approximately 50% for the 0.31 g/cm3 and 70% for 0.12 g/cm^3 and 0.17 g/cm^3 had been reached. It was observed during these tests that the material had minimal transverse deflection during this plateau, and only began to noticeably increase after the stress values had begun to rise. It was hypothesized that the microstructure of the PUA had started to collapse at the yield stress and continued to collapse until the porosity of the material had been reduced to near zero, which is supported by the SEM images in Figure 3.10 taken after testing the material. Specimens were examined after testing and it was noted that they had become semi-translucent and spiderweb-like cracks were evident in the 0.31 g/cm^3 samples, as seen in Figure 3.11. Results from testing have been tabulated and can be seen in Table 3.2.

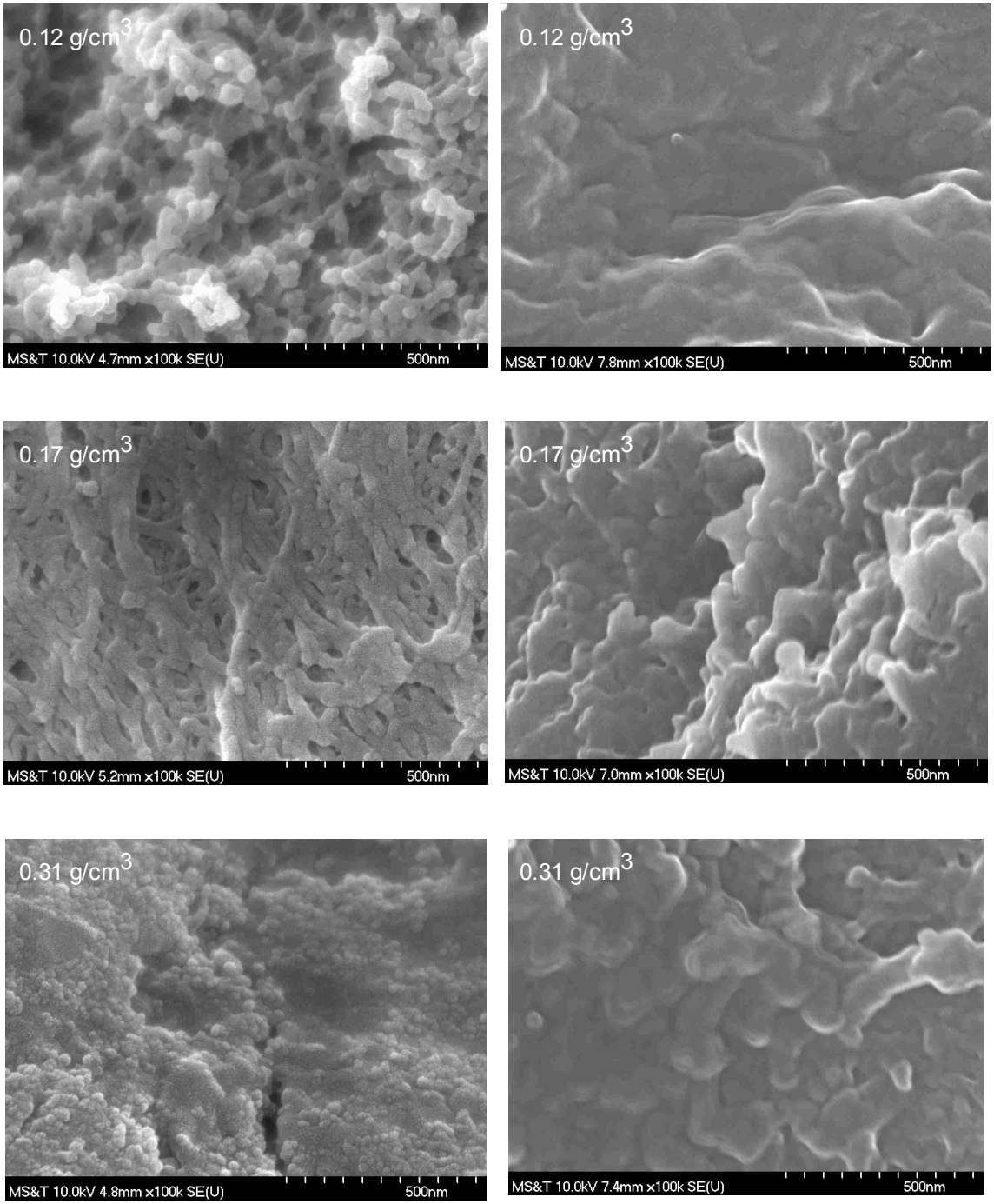

Figure 3.10. SEM Images Before and After Compression. The left column above shows the SEM images of PUA samples prior to testing and the adjacent pictures on the right show the same density samples after testing had been conducted. The top row shows 0.12 g/cm^3 PUA, middle shows 0.17 g/cm^3, and bottom shows 0.31 g/cm^3. The gaps between fibers and particles apparent before testing have been completely collapsed.

Figure 3.11. Compressive Test Specimen After Testing. The specimen has been compacted to approximately 10% of its original height. Plastic deformation to this extent has reduced the size of the gaps between adjacent microstructures leaving the material semi-translucent. A few cracks are evident, though the specimen remains intact.

Table 3.2. Compressive Testing Results

PUA Density	Young's Modulus (MPa)	Yield Stress (MPa)
0.12 g/cm ^{3}	11.7 ± 4.4	0.4 ± 0.01
0.17 g/cm ^{3}	19.3 ± 4.2	0.7 ± 0.1
0.31 g/cm ^{3}	69.0 ± 17.9	2.4 ± 0.3

3.3. BENDING

ASTM D790 is the standard test method for testing the flexural properties of reinforced and unreinforced plastics and has been chosen as the guideline for determining flexural properties of PUA. The dimensions of the test specimens given in the test method are shown in Figure 3.12 below. Five specimens have been tested at ambient conditions and the recommended strain rate of 1 mm/mm/min was used. Figure 3.13 shows the three point bend test setup with a sample loaded into the Instron material testing machine.

The results for three point bend testing have been analyzed and plotted on stress-strain curves. Figure 3.14 shows the results of testing plotted up to 5% strain, which is the prescribed stopping criteria listed in the test method. Figure 3.15 shows the same curves up to 2% strain to better observe the differences in stiffness.

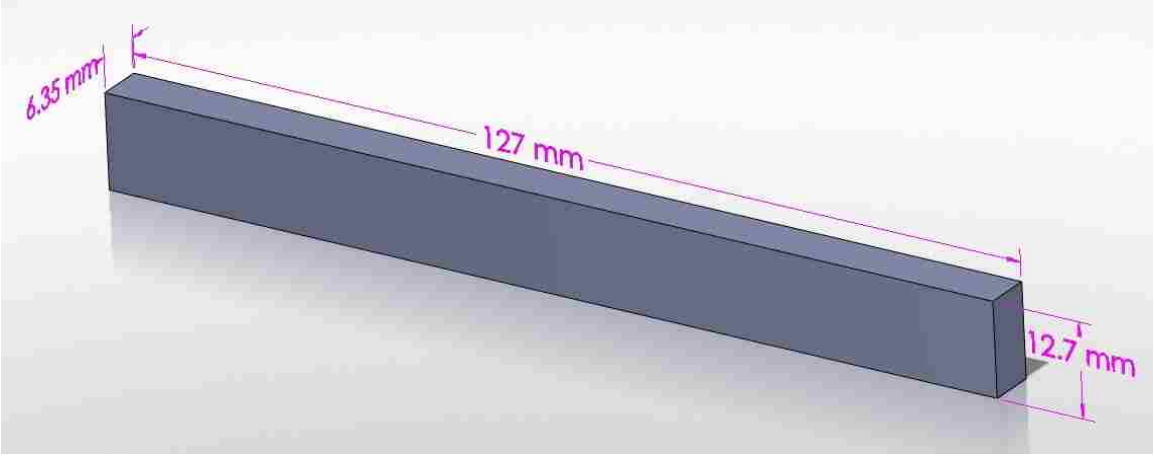

Figure 3.12. Three Point Bend Test Specimen Dimensions. The dimension of the flexural test specimens listed in the test method are indicated above.

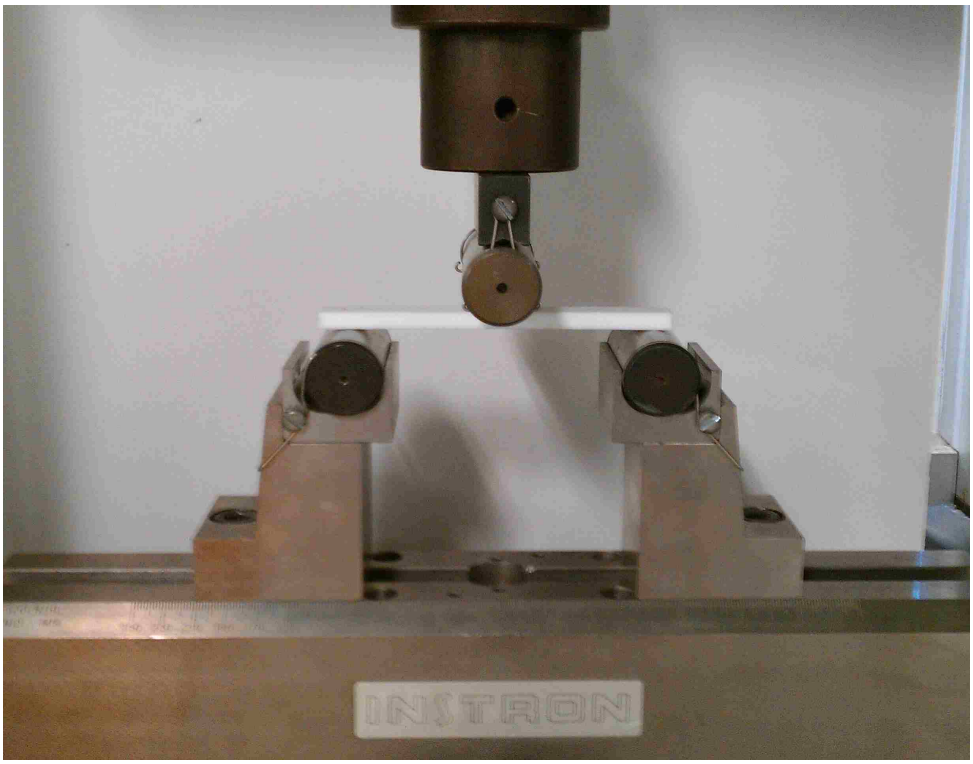

Figure 3.13. Three Point Bend Test Setup. The Instron machine has been fitted with two stationary supports with a specified span between them. The specimen is loaded by a third member attached to a load cell.

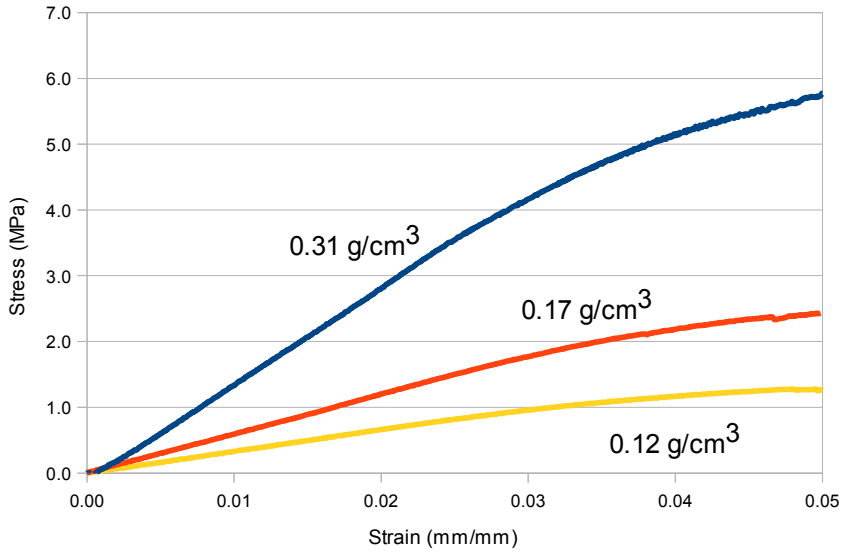

Figure 3.14. Three Point Bend Results. Above are the stress-strain results from flexural testing PUA. The top line (blue) represents the 0.31 g/cm^3 density, the middle (orange) line represents 0.17 g/cm^3, and the bottom (yellow) line is 0.12 g/cm^3.

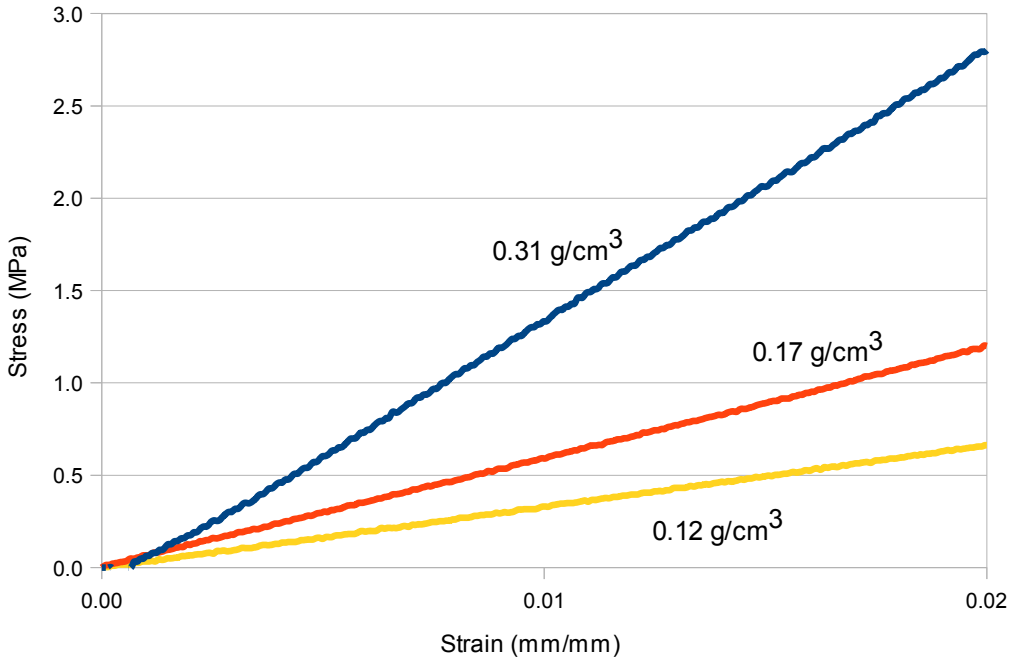

Figure 3.15. Stiffness in Flexural Results. The top line (blue) represents 0.31 g/cm^3 PUA, the middle (orange) line is 0.17 g/cm^3, and the bottom (yellow) line is 0.12 g/cm^3.

Three point bend results show that the material gains strength faster than it gains density in all cases. As in tensile and compression tests, yielding takes place at approximately 3.5% strain. None of the densities failed before 5% strain, and in accordance with the test method the results should regarded as informational only and not used for strength or stiffness calculations during the design phase of a product or part. Regardless, the results from testing have been tabulated and presented in Table 3.3.

Table 3.3. Flexural Testing Results

PUA Density	Young's Modulus (MPa)	Yield Stress (MPa)
0.12 g/cm ^{3}	33.1 ± 2.5	1.03 ± 0.1
0.17 g/cm ^{3}	62.7 ± 6.4	1.9 ± 0.1
0.31 g/cm ^{3}	137.9 ± 13.1	4.65 ± 0.4

3.4. SHEAR

Due to the recommendation listed in the ASTM test method for bending to disregard values determined from samples that showed no failure before 5% strain more testing was needed. Bending strength can be calculated if values are known for tension, compression, and shear strength. Tension and compression have been successfully investigated so it became necessary to test the properties in shear. Unlike the previous tests no ASTM standard was found for the determination of material properties in shear, thus an appropriate test had to be developed.

The method devised to exert a shear force on the PUA being tested was chosen for its simplicity A square piece of material in placed in an apparatus such that one edge has a surface traction pulling in one direction and the opposite edge has a surface traction pulling in the opposite direction. Figure 3.16 depicts the specimen and the location and direction of the forces being applied. To accomplish this aluminum tabs were glued to opposite sides of the PUA specimens. Assembled samples are shown in Figure 3.17, and Figure 3.18 shows the specimen loaded into the Instron test machine.

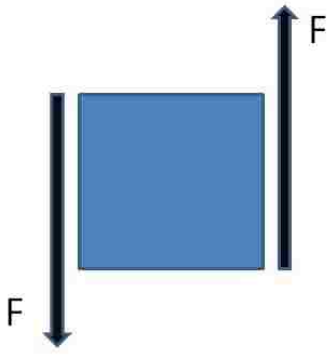

Figure 3.16. Shear Test Specimen and Force Vectors. The arrows on either side of the specimen show a surface traction on opposite sides pulling in opposite directions.

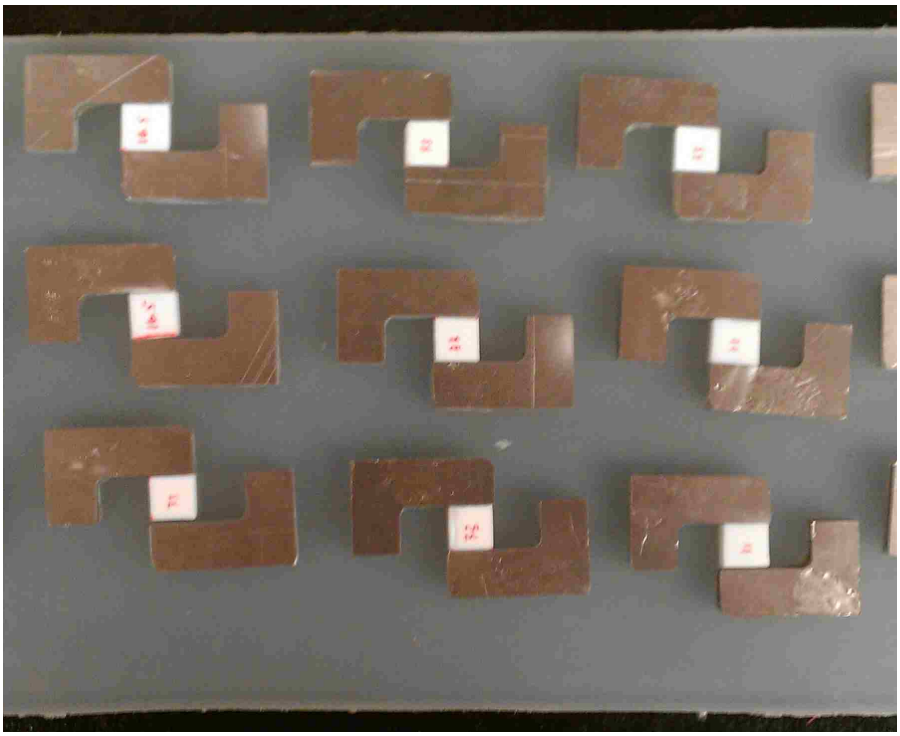

Figure 3.17. Assembled Shear Samples. Aluminum L brackets were machined using the University waterjet and adhesively bonded to the PUA samples in the center.

3.18. Shear Test Setup. The aluminum L brackets are clamped into the grips used for tensile testing.

The results for shear testing have been analyzed and plotted. Figures 3.19 shows the stress-strain curves for PUA in shear up to failure, and Figure 3.20 shows stress-strain plots for PUA up to 2% strain to better see the differences in stiffness.

Similar to the results found for tensile and compressive properties, the gain in strength and stiffness versus the gain in density appears to be a linear relationship between the lower two densities, whereas the increase to 0.31 g/cm3 density yielded an exponential gain. Testing was carried out until the specimens failed, which occurred just past 10% strain for all samples. In all cases fracture occurred at the corners of the specimen in which the deflection would cause the right angle of the corner to decrease, an example of such failure is shown in Figure 3.21. To determine if this type of failure was valid, as opposed to being caused by manufacturing or other error, a finite element model was constructed of a generic material in which the same boundary conditions and loads found in the real test were applied. The results of this study showed that the fracture in question occurred at the point of highest stress, showing that the actual specimens failed as they should have. Figure 3.22 shows the finite element model used. The results of shear testing have been tabulated and are presented in Table 3.4.

Table 3.4. Shear Testing Results

PUA Density	Shear Modulus (MPa)	Yield Stress (MPa)	Failure Stress (MPa)
0.12 g/cm^3	8.3 ± 0.6	0.2 ± 0.02	0.4 ± 0.03
0.17 g/cm^3	11.7 ± 0.7	0.4 ± 0.04	0.7 ± 0.08
0.31 g/cm^3	37.9 ± 2.5	1.2 ± 0.2	1.6 ± 0.3

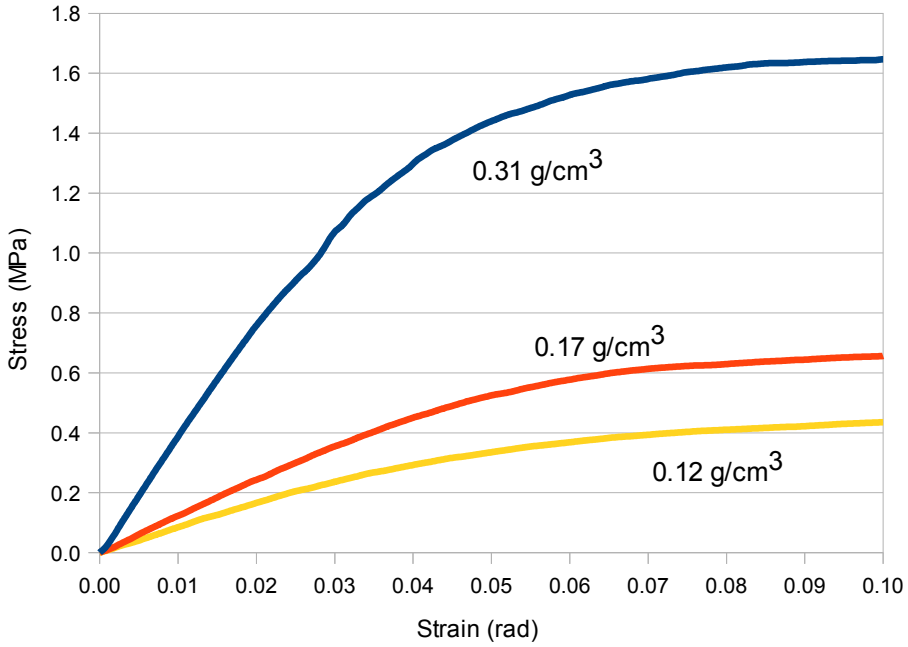

Figure 3.19. Shear Test Results. The stress-strain curves for shear testing are shown above. The top (blue) line represents the 0.31 g/cm^3 density, the middle (orange) line 0.17 g/cm^3, and the bottom (yellow) 0.12 g/cm^3. Failure of all three samples occurred just past 10% strain.

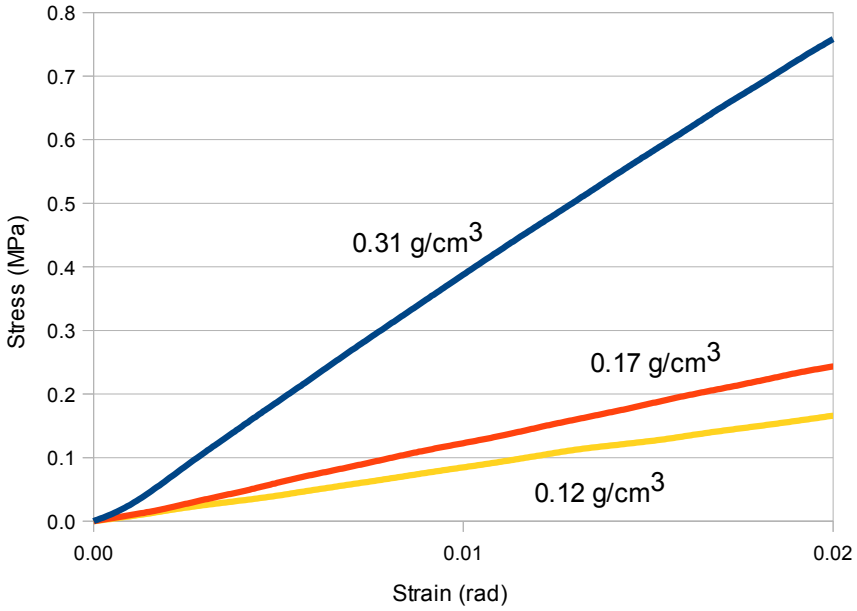

Figure 3.20. Stiffness in Shear Results. The above stress-strain curves show the difference in stiffness between the three densities. The top (blue) line represents 0.31 g/cm^3, the middle (orange) line 0.17 g/cm^3, and the bottom (yellow) line 0.12 g/cm^3.

Figure 3.21. Failed Shear Sample. The above figure shows the fractures in the sample (circled in red) shortly after testing.

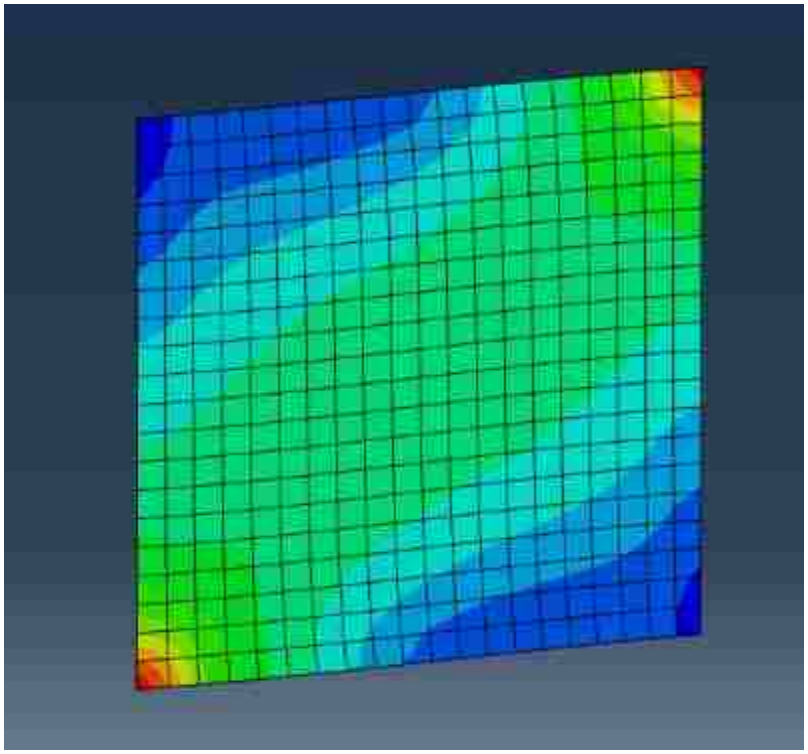

Figure 3.22. Finite Element Model of Shear Test Specimen. Finite element analysis was used to determine the areas of highest stress within the PUA samples. The red corners (upper right and lower left) show areas of particularly high stress which supports the observations made during testing.

3.5. CHARPY IMPACT

The previous four tests represent much of what is needed to design a structural part in terms of strength and stiffness. They, however, only deal with said part in a quasi-static environment. Impact testing was chosen to investigate the toughness of PUA. ASTM D6110 prescribes the standard test method for the determination of Charpy impact resistance for notched specimens of plastic and has been used as a guide for PUA testing. Test setup and specimen dimensions are prescribed by the test method and have been adhered to. Figure 3.23 shows the specimen dimensions used for this test. Figure 3.24 shows the Charpy impact machine used for testing.

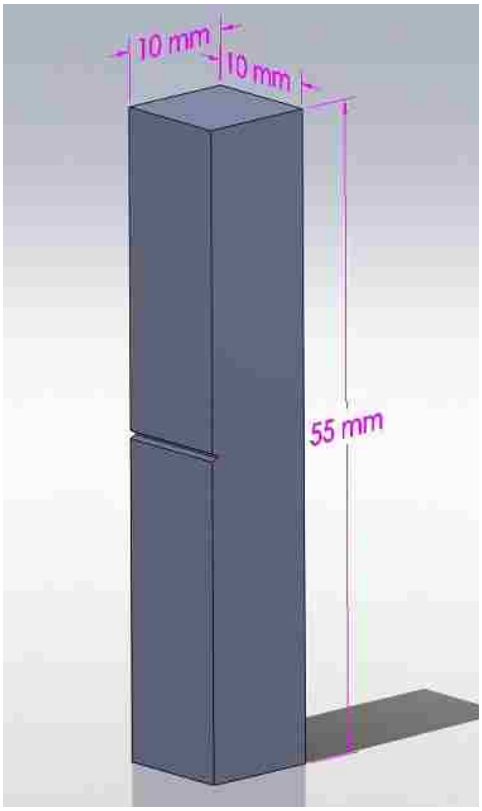

Figure 3.23. Charpy Test Specimen Dimensions. The major dimensions of the specimens used for Charpy impact testing are shown above.

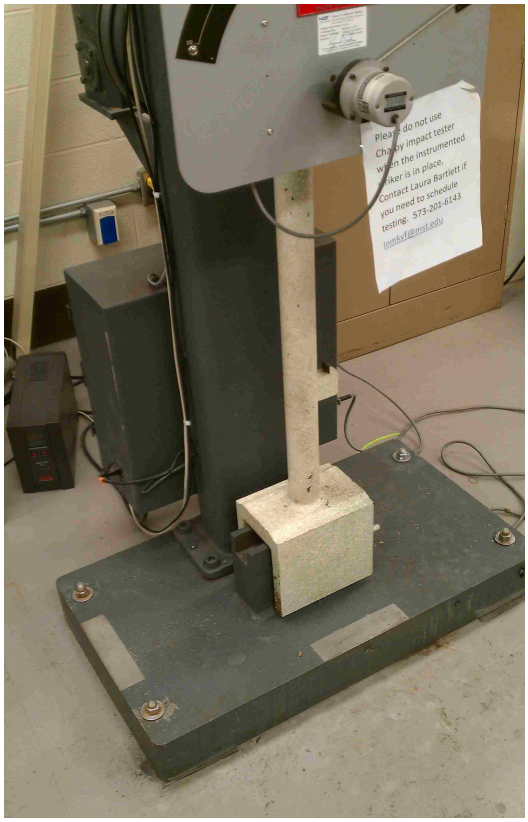

Figure 3.24. Charpy Impact Test Setup. Specimens to be used for Charpy impact testing are placed between the two steel uprights seen in the center of the base of the machine. The striking hammer (white, center of figure) is then raised and swung through the specimen. Energy absorbed during the impact is displayed on a digital readout.

The results from Charpy impact testing show that the highest density tested, 0.31 g/cm^3, was able to absorb more energy that either of the two lower densities, though it was unable to register a value higher than the error tolerance of the machine. The output of the test are in units of foot-pounds, and the testing machine's error tolerance is ± 1 foot-pound. Testing 0.31 g/cm^3 samples yielded an average result of 0.1 ft-lbs, while the 0.12 g/cm^3 and 0.17 g/cm^3 samples both averaged 0.05 ft-lbs. Because the results are lower than the error tolerance of the testing machine they should only be used for comparison to each other and not for calculations regarding toughness.

4. DISCUSSION OF RESULTS AND CONCLUSIONS

The results from testing have been compiled and are presented in Table 4.1. As it was noted in Section 3.3, the results from bending are informational only and should not be used in calculations for strength or stiffness, although with the combined results from tension, compression, and shear testing the bending strength and stiffness can be calculated.

Table 4.1. Compiled Results

Tension	PUA Density	Young's Modulus (MPa)	Yield Stress (MPa)	Failure Stress (MPa)	Failure Strain (%)
	0.12 g/cm^3	24.1 ± 0.5	0.7 ± 0.03	1.1 ± 0.08	12.5 ± 2.3
	0.17 g/cm^3	37.2 ± 1.3	1.0 ± 0.2	1.7 ± 0.1	13.5 ± 3.0
	0.31 g/cm^3	102 ± 7.2	2.9 ± 0.4	3.9 ± 0.2	6 ± 0.6
Compression	PUA Density	Young's Modulus (MPa)	Yield Stress (MPa)		
	0.12 g/cm3	11.7 ± 4.4	0.4 ± 0.01		
	0.17 g/cm3	19.3 ± 4.2	0.7 ± 0.1		
	0.31 g/cm3	69.0 ± 17.9	2.4 ± 0.3		
Bending	PUA Density	Young's Modulus (MPa)	Yield Stress (MPa)		
	0.12 g/cm3	33.1 ± 2.5	1.03 ± 0.1		
	0.17 g/cm3	62.7 ± 6.4	1.9 ± 0.1		
	0.31 g/cm3	137.9 ± 13.1	4.65 ± 0.4		
Shear	PUA Density	Shear Modulus (MPa)	Yield Stress (MPa)	Failure Stress (MPa)	
	0.12 g/cm3	8.3 ± 0.6	0.2 ± 0.02	0.4 ± 0.03	
	0.17 g/cm3	11.7 ± 0.7	0.4 ± 0.04	0.7 ± 0.08	
	0.31 g/cm3	37.9 ± 2.5	1.2 ± 0.2	1.6 ± 0.3	

The above results will prove useful for preliminary design of structures under static loads with stresses less then the material's yield stress. Structures under dynamic loads or in extreme environments (very hot/cold, moist, etc) would require additional testing. Some of such tests include fatigue and creep testing to determine how PUA would react under various long term conditions. Dynamic mechanical analysis will also prove useful for determining strength and stiffness at varying strain rates and temperatures.

PUA has proven to be mechanically strong, especially in terms of strength to weight, though its true strength is in its ability to take extreme loads in compression. 0.31 g/cm^3 PUA was able to support forty thousand times its own weight in compression at its yield and over three million times its own weight at its highest strain values. It appears that PUA is well suited to applications that require low weight, high strength, and high strain, as long as it is only necessary to perform once. An application that comes immediately to mind is any variety of impact absorbing structures such as those found in automobiles or race cars. Assuming processes could be developed to keep production and manufacturing costs to a minimum, PUA could prove to be an incredibly useful new material used to advance a wide variety of engineered structures.

BIBLIOGRAPHY

[1] Chakkaravarthy, C., Larimore, Z., Sotiriou-Leventis, C., Mang, J., & Leventis, N. (2010). One-Step room-temperature synthesis of fibrous polyimide aerogels from anhydrides and isocyanates and conversion to isomorphic carbons. *Journal of Materials Chemistry,* (vol 20, p 9666-9678)

[2] Leventis, N., Sotiriou-Leventis, C., Chandrasekaran, N., Mulik, S., Larimore, Z., Lu, H., Churu, G.,Mang, T. (2010) Multifunctional Polyurea Aerogels from Isocyanates and Water. A Structure-Property Case Study. *Chemistry of Materials*, (vol 22, p 6692-6710)

[3] Kistler, S. (1932) Coherent Expanded Aerogels. *Journal of Physical Chemistry.* (vol 36, p 52-64)

[4] History of Silica Aerogels. April 2004. Environmental Energy Technologies Division, Lawrence Berkeley National Laboritory. 25 August 2011. <http://eetd.lbl.gov/ecs/aerogels/>

[5] Zhang, G., Dass, A., Rawashdeh, A., Thomas, J., Counsil, J., Sotiriou-Leventis, C., Fabrizio, E., Ilhan, F., Vassilaras, P., Scheiman, D., McCorkle, L., Palczer, A., Johnston, J., Meador, M., Leventis, N. (2004) Isocyanate-Crosslinked Silica Aerogel Monoliths: Preparation and Characterization. *Journal of Non-Crystalline Solids.* (vol 350, p 152-164)

[6] Leventis, N., Palczer, A., McCorkle, L. (2005) Nanoengineered Silica-Polymer Composite Aerogels with No Need for Supercritical Fluid Drying. *Journal of Sol-Gel Science and Technology.* (vol 35, p 99-105)

[7] Lee, J., Gould, G., Rhine, W. (2009) Polyurea Based Aerogel for a High Performance Thermal Insulation Material. *Journal of Sol-Gel Science and Technology.* (vol 49, p 209-220)

[8] Roy, S., Shimpi, N., Katti, A., Lu, H., Rahman, M. (2006) Mechanical Characterization and Modeling of Isocyanate-Crosslinked Nanostructured Silica Aerogels. 47th *AIAA/ASM/ASCE/AHS/ASC Structures, Structural Dynamics, and Materials Conference.*

[9] Reinheimer, Preston Glenn. *Construction of a Multi-Functional Cryogenic Propellant Tank with Cross Linked Silica Aerogel*. MS Thesis. University of Alabama, Tuscaloosa, 2010. ProQuest Dissertations and Theses. Web. 25 August 2011.

[10] Leventis, N., Sotiriou-Leventis, C., Zhang, G., Rawashdeh, A. (2002) Nanoengineering Strong Silica Aerogels. *Nano Letters.* (vol 2, p 957-960)

[11] Capadonaa, L., Meador, M., Alunni, A., Fabrizio, E., Vassilaras, P,. Leventis, N. (2006) Flexible, Low-Density Polymer Crosslinked Silica Aerogels. *Polymer,* (vol 47, p 5754-5761)

[12] Bian, Q., Chen, S., Kim, B., Leventis, N., Lu, H., Chang, Z., Lei, S. (2011) Micromachining of Polyurea Aerogel Using Femtosecond Laser Pulses. *Journal of Non-Crystalline Solids* (vol 357, p 186-193)

[13] Philpot, Timothy A., Mechanics of Materials: An Integrated Learning System. Wiley, 2008

[14] "Standard Test Method for Tensile Properties of Plastics," ASTM D638, American Society for Testing and Materials, 2010.

[15] "Standard Test Method for Compressive Properties of Rigid Plastics," ASTM D695, American Society for Testing and Materials, 2010.

[16] "Standard Test Methods for Flexural Properties of Unreinforced and Reinforced Plastics and Electrical Insulating Materials," ASTM D790, American Society for Testing and Materials, 2010.

[17] "Standard Test Method for Determining the Charpy Impact Resistance of Notched Specimens of Plastics," ASTM D6110, American Society for Testing and Materials, 2010.

VITA

Jared Michael Loebs was born in Frankfurt, Germany to parents Peter Michael Loebs, a Captain in the US Army, and Rainee Lynn Loebs, a Registered Nurse. Jared received secondary education in St. Charles, Missouri and graduated from Francis Howell North High School in May of 2005. In the fall of the same year Jared was admitted to the University of Missouri – Rolla where he participated in many extra-curricular activities including becoming a member of Kappa Alpha Order and serving as the Chief Engineer for the Advanced Aero Vehicle Group for three years. In May 2009 Jared graduated from the newly renamed Missouri University of Science and Technology with a Bachelor of Science degree in Aerospace Engineering, minoring in Material Science.

After receiving a Bachelor's degree Jared decided to continue his education at Missouri S&T and started on a M.S. degree in Mechanical Engineering in the Fall of 2009. While pursuing his degree Jared has worked as a Graduate Teaching Assistant where he taught IDE20, as well as a Graduate Research Assistant in the Leventis Labs.

Jared will receive his Master of Science degree in the Fall of 2011.